JBC Papers in Press. Published on March 29, 2011 as Manuscript M111.224832
The latest version is at http://www.jbc.org/cgi/doi/10.1074/jbc.M111.224832

Characterization of NocL Involved in Thiopeptide Nocathiacin I Biosynthesis: A [4Fe-4S] Cluster and the Catalysis of a Radical S-Adenosylmethionine Enzyme

Qi Zhang[‡1], Dandan Chen[§‡1], Jun Lin[¶], Rijing Liao[‡], Wei Tong[‖], Zhinan Xu[§], and Wen Liu[‡2]

From the [‡]State Key Laboratory of Bioorganic and Natural Products Chemistry, Shanghai Institute of Organic Chemistry, Chinese Academy of Sciences, Shanghai 200032, China; the [§]Department of Chemical Engineering and Biotechnology, Zhejiang University, Hangzhou 310027, China; the [¶]Shanghai Institute of Applied Physics, Chinese Academy of Sciences, Shanghai, 201800, China; and the [‖] High Magnetic Field Laboratory, Chinese Academy of Sciences, Hefei, Anhui 230031, China.

Running Title: Characterization of NocL as a radical SAM MIA synthase

[1]These author contributed to this work equally.
[2]To whom correspondence should be addressed: Wen Liu, Shanghai Institute of Organic Chemistry, Chinese Academy of Sciences, 345 Lingling Rd., Shanghai 200032, China. Email: wliu@mail.sioc.ac.cn, Tel: 86-21-54925111, Fax: 86-21-64166128.

The radical S-adenosylmethionine (SAM) enzyme superfamily is remarkable at catalyzing chemically diverse and complex reactions. We have previously shown that NosL, which is involved in forming the indole side ring of the thiopeptide nosiheptide, is a radical SAM enzyme that processes L-Trp to afford 3-methyl-2-indolic acid (MIA) via an unusual fragmentation-recombination mechanism. We now report the expansion of the MIA synthase family by characterization of NocL, which is involved in nocathiacin I biosynthesis. EPR and UV-Vis absorbance spectroscopic analyses demonstrated the interaction between L-Trp and the [4Fe-4S] cluster of NocL, leading to the assumption of non-specific interaction of [4Fe-4S] cluster with other nucleophiles via the unique Fe site. This notion is supported by the finding of the heterogeneity in the [4Fe-4S] cluster of NocL in the absence of SAM, which was revealed by the EPR study at very low temperature. Furthermore, a free radical was observed by EPR during the catalysis, which is in good agreement with the hypothesis of a glycyl radical intermediate. Combined with the mutational analysis, these studies provide new insights into the function of the [4Fe-4S] cluster of radical SAM enzymes, as well as the mechanism of the radical-mediated complex carbon chain rearrangement catalyzed by MIA synthase.

Fe-S clusters are ubiquitous and ancient prosthetic groups that are essential for a wide range of biological processes (1-4). Besides their most prominent function of mediating electron transfer, another important role of Fe-S cluster is their direct interaction with the substrates in various enzymatically redox or non-redox reactions. The best characterized non-redox reaction of a Fe-S cluster is aconitase, an enzyme in the citric acid cycle that utilizes a [4Fe-4S] cluster as a Lewis acid to activate the substrate (5). Enzymes catalyzing redox reactions, on the other hand, show remarkable versatility. These include the emerging large class of radical S-adenosylmethionine (SAM) enzymes that perfom the catalysis with SAM through a radical-associated mechanism (6-10).

Since the discovery of the first member, lysine 2, 3-aminomutase in 1970 (11), the radical SAM superfamily is now believed to comprise of thousands of proteins that participate in numerous biochemical processes in animals, plants, and microorganisms. These enzymes contain a motif of three cysteine residues (usually as CxxxCxxC) that nucleate a [4Fe-4S] cluster for binding of SAM via a unique Fe (Fe_u) site uncoordinated to the cysteine residue. A common mechanism is shared for generation of a powerful reagent 5'-deoxyadenosyl radical, with the [4Fe-4S] cluster serving as an electron donor to reductively cleave the carbon-sulfur bond of SAM, thereby initiating highly diverse transformations. One fascinating aspect of radical SAM proteins is their potential to catalyze highly complex structural rearrangements, as exemplified by ThiC in thiamine biosynthesis (12) and MoaA in molybdenum cofactor biosynthesis (13, 14).

We recently demonstrated that NosL, a radical SAM enzyme involved in biosynthesis of the thiopeptide antibiotic nosiheptide (NOS, Fig. 1A), catalyzes the rearrangement of L-Trp to afford 3-methyl-2-indolic acid (MIA) (15, 16). The shunt products, 3-methylindole and glyoxylate, were produced during the *in vitro* assay. In addition, glycine, assumedly originating from a glycyl radical intermediate, was detected by using a rapid-quench and derivatization method. These results strongly support an unprecedented fragmentation-recombination strategy that is utilized for the carbon chain reconstitution of L-Trp during the catalysis (Fig. 1B).

Notably, all the NOS-like, e-series thiopeptides contain the MIA moiety (17), including nocathiacin I (NOC-I, Fig. 1A) produced by *Nocardia sp. ATCC202099* (18, 19), which represents the most pharmaceutically promising members of the thiopeptide antibiotics numbering over 80 entities reported to date. This indicates that NosL homologs might be involved in the biosynthetic pathways of all the e-series thiopeptides for the MIA moiety formation. Indeed, *nocL*, which encodes a protein with 78% identity to NosL, was identified within the biosynthetic gene cluster of NOC-I (20). Heterologous expression of *nocL* in the *nosL* deletion mutant readily restored NOS production, confirming that they are functionally interchangeable.

We now report the characterization of NocL as a radical SAM MIA synthase by *in vivo* and *in vitro* studies. EPR and UV-Vis absorbance analysis indicate that besides interacting with SAM, a fraction of [4Fe-4S] cluster of the enzyme also interact with L-Trp. Comparative analysis of EPR spectra at different temperatures revealed that the [4Fe-4S] cluster is heterogeneous in the absence of SAM, supporting the non-specific interaction of the [4Fe-4S] cluster with other nucleophiles. During the steady-state of catalysis, a free radical was observed by EPR, which is consistent with the presence of a glycyl radical as proposed previously in NosL-catalyed reaction (16). Combined with the mutational analysis, these studies provided new insights into the function of [4Fe-4S] cluster in radical SAM enzymes, as well as the mechanism of the radical-mediated carbon chain reconstitution of L-Trp catalyzed by MIA synthase.

Experimental Procedures

Materials—Biochemicals and media were purchased from Sinopharm Chemical Reagent Co. Ltd. or Oxoid Ltd.. Restriction enzymes were from TaKaRa Biotechnology Co. Ltd.. Chemicals were from Sigma-Aldrich Co. Ltd. except L-[$^{2}H_{8}$]-Trp and L-[1-^{13}C]-Trp, which were purchased from Cambridge Isotope Laboratory Co. Ltd..

DNA Isolation, Manipulation, and Sequencing—DNA isolation and manipulation in *E. coli* were carried out according to standard

methods (21). PCR amplifications were carried out on an Authorized Thermal Cycler (Eppendorf AG 22331 Hamburg, Germany) using either Taq DNA polymerase or PfuUltra^{TM} High-Fidelity DNA polymerase. Primer synthesis and DNA sequencing were performed at the Shanghai Invitrogen Biotech Co. Ltd. and Chinese National Human Genome Center.

Sequence analysis—Protein comparison was carried out by available BLAST methods (http://www.ncbi.nlm.nih.gov/blast/). Amino acid sequence alignment was performed by the CLUSTALW method, and the DRAWTREE and DRAWGRAM methods, respectively, from BIOLOGYWORKBENCH 3.2 software (http://workbench.sdsc.edu).

Production and Activity Assay of NocL—A 1.2 kb PCR product containing *nocL* was amplified by PCR using the primer pairs 5'- A CAT ATG GCG GAA TAC CCC GG-3' (NdeI site underlined) and 5'- A GAA TTC TCA GCC GAT CGG GAT GAC G-3' (EcoRI site underlined) from pSL5001, a pOJ446-based *Nocardia sp.* ATCC202099 genomic library cosmid that contains the NOC-I biosynthetic gene cluster (20), and then cloned into pMD18-T vector (TaKaRa Biotechnology Co. Ltd.) to yield pSL4150. After sequencing to confirm the fidelity, the 1.2 kb NdeI/EcoRI fragment was recovered from pSL4150 and ligated into the same site of pET28a, making the recombinant construct pSL4151 for expressing *nocL* to give the *N*-terminal 6 x His-tagged protein. Expression, purification, reconstitution, and *in vivo* and *in vitro* activity assay of NocL were all performed as previously described for NosL (16). The quantification of Fe and labile S per molecule of the protein was performed in triplicate according to the methods described previously (22, 23)

Preparation of EPR Samples for Analyzing the Fe-S Cluster—Four aliquots of 250μL solution containing 100mM NaCl, 10 mM DTT and 100μM reconstituted NocL in 50 mM MOPS buffer (pH 8.0) were placed in the microtubes. Reagents were added to each tube in the order shown to give the following final concentrations: MOPS buffer (pH 8.0, control), sodium dithionite (2mM), sodium dithionite (2mM) and SAM (1mM), or sodium dithionite (2mM) and L-Trp (1mM). After mixing by pipette, each sample was loaded into a quartz EPR tube, frozen in liquid nitrogen and then stored on dry ice before recording the spectra.

Preparation of EPR Samples for Analyzing the Free Radical—Sample were prepared containing 100mM NaCl, 10 mM DTT, 5 mM dithionite, 2 mM SAM, and 100μ M reduced NosL in 50 mM MOPS buffer (pH 8.0) in a total volume of 900μL, which was divided into three aliquots. L-Trp, L-[$^{2}H_{8}$]-Trp or L-[1-^{13}C]-Trp was added to each solution to a final concentration of 1mM. The samples were transferred to EPR tubes, and after 3 min of incubation at the room temperature the solutions were quickly frozen in liquid nitrogen and then stored on dry ice before recording the spectra.

EPR Spectroscopy—EPR spectra were obtained at X-band using a Bruker EMX plus 10/12 spectrometer system (Bruker Co., Ltd., Germany), equipped with an Oxford ESR910 liquid helium continuous flow cryostat (Oxford-instrument Co., Ltd, UK). Acquisition conditions for the Fe-S cluster analysis are: microwave frequency, 9.390 GHz; microwave power, 1 milliwatts; field modulation amplitude, 5 Gauss; modulation frequency, 100 kHz; temperature, 13K or 2K. Acquisition conditions for free radical analysis are: microwave frequency, 9.390 GHz; microwave power, 10 microwatts; field modulation amplitude, 2 Gauss; modulation frequency, 100 kHz; temperature, 77K. EPR spectra of the iron-sulfur clusters were simulated by SimFonia (Bruker, Co., Ltd., Germany).

UV-Vis Absorbance Analysis—Samples were prepared as described above for the EPR analysis of the Fe-S cluster. The samples were

diluted 5-folds with MOPS buffer (pH 8.0) before transfer into a cuvette sealed with rubber septa for UV-Vis analysis. The protein concentration was kept the same in all the samples. To obviate the possible effect of cuvette difference, baseline corrections were performed before recording each spectrum.

Site-Specific Mutagenesis for Expressing Mutant NocL—The recombinant plasmid pSL4150 (pMD-18T derivative) that contains a 1.2 kb fragment encoding NocL serves as the template. PCR amplifications were carried out, by using the primer pair 5'-GAC TCC GAG TGC AAG TAT TGC TCG ATG CGC AAG GGC-3' and 5'-CTT GCG CAT CGA GCA ATA CTT GCA CTC GGA GTC GCA G-3' for mutation of M96 to Tyr; the primer pair 5'-C TGC ACA CG TTC GTC GCG CTC TAC ACG ACC AAC CAC TGC GAC-3' and 5'-GTT GGT CGT GTA GAG CGC GAC GAA CGT GTG CAG CCG GGG CG-3' for mutation of P83 to Ala; the primer pair 5'-GGC TTC CTC ACC GGC GCG TAC GAG GAC AAG TAC ACC C-3' and 5'-GTA CTT GTC CTC GTA CGC GCC GGT GAG GAA GCC GAC G-3' for mutation of E138 to Ala; the primer pair 5'-CGC TAC GTC AAC CCC GCT GTC CTC ATC GGA CTG CAC C-3' and 5'-CAG TCC GAT GAG GAC AGC GGG GTT GAC GTA GCG GAA C-3' for mutation of G243 to Ala; the primer pair 5'- C GTC AAC CCC GGT GTC GCC ATC GGA CTG CAC CTG G-3' and 5'- C CAG GTG CAG TCC GAT GGC GAC ACC GGG GTT GAC G-3' for mutation of L245 to Ala; and the primer pair 5'-CCC GGT GTC CTC ATC GCA CTG CAC CTG GAT GTG GCC G-3' and 5'-CAC ATC CAG GTG CAG TGC GAT GAG GAC ACC GGG G-3' for mutation of G247 to Ala. Exchanged nucleotides are underlined. After sequencing to confirm the fidelity, the mutant DNA fragments were cloned individually into pET28a, yielding the recombinant constructs for producing NocL mutants (i.e. pSL4153 for P83A, pSL4155 for M96Y, pSL4157 for E138A, pSL4159 for G243A, pSL4161 for L245A, and pSL4163 for G247A). The recombinant strain SL4151, which produces the native NocL, was utilized as the positive control in the parallel analytic process.

Results and Discussion

Identification of NocL as a radical SAM MIA synthase—nocL was cloned and ligated in pET28a followed by introduction into *E. coli* BL21 (DE3), yielding the recombinant strain SL4151 that produces NocL in an *N*-terminally 6 x His-Tagged form. HPLC-MS analysis of the culture broth of SL4151 revealed the production of MIA, with a yield (44 ± 4 mg/l) similar to that of the recombinant strain SL4101 for expressing NosL (42 ± 5 mg/L) (Fig. 2A, i, ii). MIA production was not detected in the control strain SL4100 carrying the pET28a vector alone (Fig. 2A iii), indicating that NocL is a MIA synthase.

Active NocL was then obtained by purification and reconstitution under the strictly anaerobic conditions where O_2 concentration was less than 5 ppm, yielding a sample in a dark brown color characteristic of Fe-S cluster-containing proteins. Quantitative analysis (22, 23) revealed that each moles of the protein contained 4.8 ± 0.4 moles of Fe and 4.4 ± 0.3 moles of labile S, indicating that the enzyme contains an active [4Fe-4S] cluster. Indeed, NocL was shown to produce MIA and 3-methylindole (a shunt product arising from reduction of the 3-methyleneindole intermediate) *in vitro* after addition of the reductant sodium dithionite and the substrates SAM and L-Trp. Each assay (20μM NocL, 0.5mM SAM and 0.5mM L-Trp) produced 36 ± 3 μM of MIA, with the ratio of MIA to 3-methylindole typically around 1:3 when 500μM dithionite was used (Fig. 2A, iv). This ratio dramatically decreased to about to 1: 8 when dithionite concentration was increased to 4 mM (Fig. 2A, v). The reaction does not proceed in the absence of SAM

(Fig. 2A, vi), indicating its SAM-dependence. 5'-deoxyadenosine, the trademark of radical SAM protein was also detected in the reaction. Although 5'-deoxyadenosine was produced in the absence of L-Trp, the yield was substantially enhanced by addition of L-Trp to the reaction mixture (Fig. 2B). Together, these results firmly established that NocL is a radical SAM protein that catalyzes the conversion of L-Trp to MIA in a fashion similar to that of NosL.

Interaction of the [4Fe-4S] cluster of NocL with L-Trp—EPR analysis of the reconstituted NocL resulted in a silent spectrum (Fig. 3, i), in accordance with a diamagnetic $[4Fe\text{-}4S]^{2+}$ cluster. When NocL was reduced by sodium dithionite, an axial spectrum with a g value of 2.02 and 1.91 was observed, closely resembling those of NosL and other radical SAM proteins (Fig. 3, ii). Addition of SAM to the reduced protein resulted in a rhombic spectrum with a g tensor of 2.01, 1.89 and 1.80 (Fig. 3, iii). The conversion of axial to rhombic symmetry is quite common in the radical SAM superfamily (24, 25), a likely explanation of this may due to the loss of near C3 symmetry of the [4Fe-4S] cluster by binding of SAM (Fig. 4).

Surprisingly, addition of L-Trp also led to a significant change of the spectrum (Fig. 3, v). This finding is distinct from a previous study showing that addition of substrate L-Tyr to ThiH, a phylogenetically related protein of NocL (also discussed below), did not change the EPR signal (26). Dissection of the spectrum revealed two types of signals: an axial signal with a g values of 2.02 and 1.91, exactly the same as the reduced NocL (Fig. 3, ii), and a rhombic signal with a g tensor of 2.02, 1.89 and 1.85. This indicates that only part of the cluster has been changed.

Simulations of the spectra further supported this result, showing that the intensity ratio of the two signals is about 0.6:0.4 (Fig. 3, vi-viii). As shown in Fig. 4, the [4Fe-4S] cluster of radical SAM proteins with incomplete iron coordination or non-specific coordinations (discussed in more detail below) has an approximately C3 symmetry. This usually leads to near axial EPR spectra of radical SAM proteins despite a few exceptions, such as the pyruvate formate-lyase activating enzymes that exhibit the rhombic signals (27, 28). The significant shift in the spectrum and the emergence of a rhombic signal by addition of L-Trp to NocL strongly support the interaction of L-Trp with the [4Fe-4S] cluster, which possibly arises from binding of the nucleophilic group of L-Trp (the carboxyl or/and amino group) to the Fe_u site. For ThiH, the interaction of [4Fe-4S] cluster with substrate L-Tyr may not occur, given no signal shift was observed.

To further support the interaction between L-Trp and [4Fe-4S] cluster, UV-Vis absorbance analysis was performed. The reconstituted NocL showed a spectrum typical of radical SAM enzymes, exhibiting an obvious absorption between 350nm and 450nm (Fig. 5, A). After dithionite reduction, new absorptions emerged around 600nm and 420nm, and a sharply increased absorbance at 380nm was observed (Fig. 5, B). Addition of SAM to the reduced protein led to a weakened absorbance in the 420nm region but no apparent change in the 600nm region (Fig. 5, C), corresponding to the interaction of SAM with the [4Fe-4S] cluster. Addition of L-Trp to the protein, however, also led to a change in the spectrum, with the absorption decreased slightly in both the 420 and 600 regions (Fig. 5, D). Given that the protein concentration was maintained at the same level in all assays, this UV-Vis analysis was consistent with the EPR study described above and indicated that certain interaction of L-Trp with the [4Fe-4S] indeed had taken place, which changed the structure as well as the spectra of the [4Fe-4S] cluster.

The heterogeneity of the $[4Fe\text{-}4S]^{+}$ cluster in NocL—The findings that the [4Fe-4S] cluster of NocL interacted with L-Trp inspired us to further probe the nature of the cluster. We proposed that

the Fe_u site in [4Fe-4S] cluster is coordination-deficient. As a result, when in the absence of the natural substrate SAM, the Fe_u site could act towards other nucleophiles, including bulky solvent, small molecules in the milieu or even the residues from the protein itself (Fig. 4). In addition to the identification of interaction between the [4Fe-4S] cluster of NocL and L-Trp here, the finding of a DTT-coordinated [4Fe-4S] cluster in the MoaA crystal structure is also consistent with this proposal (29). The non-specific interactions of the [4Fe-4S] cluster of NocL with unidentified ligands may cause the heterogeneity of the cluster. Unlike that of L-Trp, however, these interactions may be very weak and consequently, the resulting heterogeneity of the [4Fe-4S] cluster might not be discerned by EPR spectroscopy under the routine conditions. To experimentally support this point, we performed comparative EPR analysis of NocL by lowering the temperature, similar to a method previously used to ascertain the heterogeneity of [4Fe-4S] cluster in coproporphyrinogen III oxidase HemN (30). We reasoned that different species in a heterogeneous system could have different characteristics such as the relaxation time, and this might lead to the change in spectrum at the lowered temperature.

To achieve a clear comparison, we decreased the EPR temperature from 13K to a very low temperature of 2K. The EPR spectra of reduced NocL at this temperature shifted dramatically, with a significantly broadened linewidth and a changed lineshape, in part due to power saturation effect. Notably, a new signal at g = 2.12 was observed (Fig. 6, A), supporting the heterogeneity of the [4Fe-4S] cluster in NocL. A similar observation is also found in the spectra of NocL in the presence of L-Trp (Fig 6, B). Intriguingly, in the presence of SAM the spectrum at 2K is quite similar to that at 13K, although linewidth broadening resulting from saturation still occurred (Fig 6, C). The g = 2.12 signal is apparently absent in the spectrum, ruling out an origin in signal dispersion or irrelevant background, and demonstrating that the nucleophiles interacting non-specifically with the [4Fe-4S] cluster are replaced by SAM in this case. These results provided the EPR data of the [4Fe-4S] cluster at very low temperature and indicated the $[4Fe\text{-}4S]^+$ cluster of NocL is heterogeneous in the absence of SAM, assumably result from the non-specific interaction of [4Fe-4S] cluster with other nucleophiles at the Fe_u site. Although the detailed nature seems obscure, the finding of these non-specific interactions of the [4Fe-4S] cluster gave insights into our understanding of radical SAM enzymes and may facilitate the design of molecular probes or inhibitors to study Fe-S cluster-containing enzymes.

Identification of a Putative Glycyl Radical—Glycyl radicals are common in biochemistry and are involved in a variety of biotransformations (31). However, the radicals identified so far usually reside on protein scaffolds while the free, unbound glycyl radical is rarely seen and to our knowledge, has not been characterized by EPR spectroscopy. We previously identified a trace amount of glycine in the NosL-catalyzed reaction by applying a rapid-quench assay (16), which was proposed to come from the glycyl radical intermediate during the catalysis. Density function theory (DFT) calculations supported this proposal, as homolysis of the Cα-Cβ bond of Trp radical leading to a glycyl radical is energetically favored over heterolysis leading to dehydroglycine. The EPR spectra of glycyl radicals characterized so far are characteristic of a 2-fold splitting caused by the nuclear hyperfine coupling of the hydrogen with the unpaired electron on Cα (32, 33). The spectra of Trp radicals, on the other hand, are anisotropic and variable in different cases (34, 35). We examined the glycyl radical and/or possibly the Trp radical during the steady-state of NocL catalysis by EPR

spectroscopy under conditions that focus on and enhance the free radical signal. The reduced NocL exhibited a very weak signal at g = 2.001, which serves as the background (Fig. 7, A). When frozen under the steady-state of catalysis, the signal intensity showed 4~5 fold enhancement, indicating the production of new radical(s) during the catalysis. Interestingly, by subtracting the background, a splitting signal centered at g = 2.0015 was found (Fig. 7, B), which correlated well with a free glycyl radical. The g value of this signal is slightly smaller than the well characterized protein-based glycyl radical usually found at g = 2.002 to 2.004 (33), possibly reflecting the difference of the radicals in the free and protein-based forms. However, as the spectrum is background-subtracted, the complex non-Gaussian lineshape might make g value determination inaccurate. Use of L-[$^{2}H_{8}$]-Trp in place of L-Trp led to the collapse of the signal into a singlet (Fig. 7, C), which may arise from the 6-fold smaller splitting constant for deuterium relative to hydrogen. Substitution of L-Trp by L-[1-^{13}C]-Trp showed significant broadening and alteration of the signal (Fig. 7, D), confirming that the radical is centered on Cα and further supporting it to be a glycyl radical. The broadened linewidth and the complex lineshape of the spectra implied that other free radicals such as a Trp radical might also exist in the assay in addition to glycyl raidcal.

Mutational Analysis of NocL—NocL and NosL both belong to the ThiH subfamily of radical SAM enzymes that cleave the Cα-Cβ bond of aromatic amino acids (26, 36, 37). Similar to other radical SAM proteins, this protein subfamily possesses a conserved CxxxCxxC motif for binding of the [4Fe-4S] cluster, a conserved "GE" motif proposed for binding of the methionine part of SAM, and a relatively conserved "GxxLxxG" motif for binding of the adenine part of SAM (Fig. 8) (38). For NosL we previously replaced each cysteine residues in the CxxxCxxC motif and the glycine residue in the "GE" motif of NosL to alanine. All the mutants lost the ability to synthesize MIA, indicating the importance of these residues to the biological activity of the MIA synthase (16).

We then performed mutational analysis of NocL to further probe the function of these conserved motifs (Fig. 9). Replacement of the glutamate residue in the "GE" motif to alanine completely abolished the ability of NocL to synthesize MIA, indicating that disruption of this SAM binding site is fatal to the catalysis. Replacing the residue in the "GxxLxxG" motif resulted different outcomes: the production of MIA was completely lost in the mutant "GxxLxxA", while it was retained in the mutants "AxxLxxG" and "GxxAxxG" despite that the yield was significantly reduced. These demonstrated that the residues selected for mutation are not as crucial as "GE" motif for SAM binding. Most of the radical SAM proteins possess the motif "CxxxCxΦC" where Φ represents aromatic amino acids (30). This is true for ThiHs and HydG, but for NocL or NosL, the aromatic acid is replaced by methionine. When replacing the methionine in the CxxxCxMC motif of NocL to tyrosine, the mutant showed a 2-fold decreased production of MIA as compared to the native enzyme, indicating that this methionine residue in NocL may not play a specific role. The decreased activity of the mutant may arise from the conformational change caused by the large p-hydroxyphenyl group of tyrosine.

We also probed the effect of conformational change to the catalytic activity. The entire protein subfamily contains a conserved proline in the middle of the first of N-terminal β-sheet (38), which may be important for protein conformation. Replacement of this residue to alanine resulted in only a 1.5-fold decrease of MIA production, indicating that the residues outside the protein active site may not be essential for the protein catalysis.

Conclusion

We have expanded the MIA synthase family by *in vivo* and *in vitro* characterization of NocL, which is involved in biosynthesis of the thiopeptide antibiotic NOC-I. The catalytic efficiency of NocL is similar to that of NosL, confirming the functional complementarity of these proteins. EPR and UV-Vis spectrometries revealed the interaction of the [4Fe-4S] cluster with L-Trp, leading to the notion of non-specific interaction of the [4Fe-4S] cluster with other nucleophiles via the Fe_u site. Comparative EPR analysis at different temperatures showed the heterogeneity of [4Fe-4S] cluster in the absence of SAM and supported the notion of non-specific interactions. Identification of these interactions will certainly contribute to future studies, not only for radical SAM proteins but also for other Fe-S containing enzymes.

The most prominent feature of MIA synthase family is the fragmentation-recombination process, in which a putative glycyl radical serves as the key intermediate during the catalysis. The EPR study here revealed the presence of this radical, supporting our previous mechanistic hypothesis (16) and paving the way for investigation into the radical chemistry of the catalytic process. Mutational analysis further demonstrated the indispensability of the conserved motif for [4Fe-4S] and SAM binding. Complete understanding of the intriguing chemistry of the radical SAM MIA synthase is awaiting future studies, such as the structural elucidation of the enzymes.

Reference

1. Johnson, M. K. (1994) *Encyclopedia of Inorganic Chemistry, King, R. B. Ed.*, pp. 1896–1915, Wiley, Chichester, UK
2. Beinert, H., Holm, R. H., and Munck, E. (1997) *Science*, **277**, 653–659
3. Beinert, H. (2000) *J. Biol. Inorg. Chem.* **5**, 2–15
4. Johnson, D. C., Dean, D. R., Smith, A. D., and Johnson, M. K. (2005) *Annu. Rev. Biochem.* **74**, 247–281
5. Beinert, H., Kennedy, M. C., and Stout, C. D., (1996) *Chem. Rev.* **96**, 2335–2373
6. Cheek, J., and Broderick, J. B. (2001) *J. Biol. Inorg. Chem.* **6**, 209–226
7. Sofia, H. J., Chen, G., Hetzler, B. G., Reyes-Spindola, J. F., and Miller, N. E. (2001) *Nucleic Acids Res.* **29,** 1097-1106
8. Frey, P. A., and Magnusson, O. T. (2003) *Chem. Rev.* **103**, 2129-2148
9. Jarrett, J T. (2003) *Curr. Opin. Chem. Biol.* **7**, 174–182
10. Frey, P. A., Hegeman, A. D., and Ruzika, F. J., (2008) *Critical. Rev. Biochem. Mol. Biol.* **43**, 63-88
11. Chirpich, T. P., Zappia, V., Costilow, R. N., Barker, H. A. (1970) *J. Biol. Chem.* **245**, 1778-1789
12. Chatterjee, A., Li, Y., Zhang, Y., Grove, T. L., Lee, M., Krebs, C., Booker, S. J., Begley, T. P., and Ealick, S. E. (2008) *Nat. Chem. Biol.* **4**, 758-765
13. Hanzelmann, P., Schwarz, G., and Mendel, R. R. (2002) *J. Biol. Chem.* **277**, 18303–18312
14. Hanzelmann, P., and Schindelin, H.(2006) *Proc. Natl. Acad. Sci. U. S. A.* **103**, 6829–6834.
15. Yu, Y., Duan, L., Zhang, Q., Liao, R., Ding, Y., Pan, H., Wendt-Pienkowski, E., Tang, G., Shen,

B., and Liu, W. (2009) *ACS Chem. Biol.* **4**, 855-864
16. Zhang, Q., Li, Y., Chen, D., Yu, Y., Duan, L., Shen, B., and Liu, W. (2011) *Nat. Chem. Biol.* **7**, 154-160
17. Bagley, M .C., Dale, J. W., Merritt, E. A., and Xiong, X. (2005) *Chem. Rev.* **105**, 685-714
18. Li, W., Leet, J. E., Ax, H. A., Gustavson, D. R., Brown, D. M., Turner, L., Brown, K., Clark, J., Yang, H., Fung-Tomc, J., and Lam, K. S. (2003) *J. Antibiot*. **56**, 226–231
19. Leet, J. E., Li, W., Ax, H. A., Matson, J. A., Huang, S., Huang, R., Cantone, J. L., Drexler, D., Dalterio, R. A., and Lam, K. S. (2003) *J. Antibiot*. **56**, 232–242
20. Ding, Y., Yu, Y., Pan, H., Guo, G., Li, Y., and Liu, W. (2010) *Mol. BioSysts.* **6**, 1180-1185
21. Sambrook, J., and Russell, D.W. (2001). *Molecular Cloning: A Laboratory Manual, Third Edition.,* Cold Spring Harbor Laboratory Press, Cold Spring Harbor, NY.
22. Beinert, H. (1983) *Anal. Biochem*. **131**, 373-378
23. Kennedy, M. C., Kent, T. A., Emptage, M., Merkle, H., Beinert, H., and Munck, E. (1984) *J. Biol. Chem.* **259**, 14463-14471
24. Liu, A., and Graslund, A. (2000) *J. Biol. Chem.* **275**, 12367–12373
25. Brindley, A. A., Zajicek, R., Warren, M. J., Ferguson, S. J., and Rigby, S. E. J. (2010) *FEBS Letters*. **584**, 2461–2466
26. Kriek, M., Martins, F., Leonardi, R., Fairhurst, S. A., Lowe, D. J, Roach, P. L. (2007) *J. Biol.Chem.* **282**, 17413-17423
27. Walsby, C., Ortillo, D., Yang, J., Nnyepi, M. R., Broderick, W. E., Hoffman, B. M., and Broderick, J. B. (2005) *Inorg. Chem.* **44**, 727-741
28. Walsby, C., Hong, W., Broderick, W. E., Ortillo, D., Broderick, J. B., and Hoffman, B. M. (2002) *J. Am. Chem. Soc*. **124**, 3143-3150.
29. Hanzelmann, P., and Schindelin, H. (2004) *Proc. Natl. Acad. Sci. U. S. A.* **101**, 12870–12875
30. Layer, G., Grage, K., Teschner, T., Schunemann, V., Breckau, D., Masoumi, A., Jahn, M., Heathcote, P., Trautwein, A. X., and Jahn, D. (2005) *J. Biol. Chem,* **280**, 29038–29046
31. Himo, F., and Siegbahn, P. E. M. (2003) *Chem. Rev.* **103**, 2421–2456
32. Sun, X., Ollagnier, S., Schmidt, P. P., Atta, M., Mulliez, E., Lepape, L., Eliasson, R., Graslund, A., Fontecave, M., Reichard, P., and Sjoberg, B. M. (1996) *J. Biol. Chem,* **271**, 6827–6831
33. Krieger, C. J., Roseboom, W., Albracht, S. P. J., Spormann, A. M. (2001) *J. Biol. Chem.* **276**, 12924-12927
34. Lendzian, F., Sahlin, M., MacMillan, F., Bittl, R., Fiege, R., Potsch, S., Sjoberg, B. M., Graslund, A., Lubitz, W., and Lassmann, G. (1996) J. Am. Chem. Soc. **118**, 8111-8120
35. Miller, J. E., Gradinaru, C., Crane, B. R., Di Bilio, A. J., Wehbi, W. A., Un, S., Winkler, J. R., and Gray, H. B. (2003) J. Am. Chem. Soc. **125**, 14220-14221
36. Kriek, M., Martins, F., Challand, M. R., Croft, A., and Roach, P. L. (2007) *Angew. Chem. Ind. Ed.* **46**, 9223-9226
37. Driesener, R. C., Challand, M. R., McGlynn, S. E., Shepard, E. M, Boyd, E. S., Broderick, J. B., Peters, J. W., and Roach, P. L. (2010) *Angew. Chem. Int. Ed.* **49**, 1687-1690
38. Nicolet, Y., and Drennan, C. L. (2004) *Nucleic Acids Res.* **32**, 4015-4025

Footnotes

*We thank Mr. John Hung, University of Illinois at Urbana-Champaign, for critical reading of the manuscript. This work was supported in part by grants from the National Natural Science Foundation (20832009, 30525001 and 20921091), the Ministry of Science and Technology (2009ZX09501-008), the National Basic Research Program ("973 program", 2010CB833200), the Chinese Academy of Sciences (KJCX2-YW-H08 and KSCX2-YW-G-06), and the Science and Technology Commission of Shanghai Municipality (09QH1402700) of China.

The abbreviations used are: MIA, 3-methyl-2-indolic acid; DFT, density function theory; NOC-I, nocathiacin I; NOS, nosiheptide; SAM, S-adenosylmethionine; Fe_u, unique Fe.

Figure Legend

Fig 1. **Structures of e-series thiopeptides NOS and NOC-I and the key step for their side ring moiety formation.** (A) NOS and NOC-I, the indolic acid moiety are shown in dash cycle. (B) The fragmentation-recombination mechanism of NocL/NosL in processing L-Trp to MIA.

Fig 2. **Characterization of NocL as a radical SAM MIA synthase.** (A) *In vivo* MIA production in the *E. coli* strains, including SL4151 harboring *nocL* (i), SL4101 harboring *nosL* (ii), and SL4100 carrying the empty vector alone (iii); and *in vitro* conversion of L-Trp to MIA and the shunt product 3-methylindole in the presence of SAM and 0.5mM (iv) or 4mM (v) sodium dithionite, with reaction in the absence of SAM as the control (vi). (B) Conversion of SAM to 5'-deoxyadenosine in the absence (i) and the presence of L-Trp (ii), in contrast to that by omitting NocL from the reaction mixture (iii). The solid diamond indicated an unidentified metabolite that is independent of MIA production.

Fig 3. **X-band EPR spectra of reconstituted NocL for Fe-S cluster characterization.** Bold lines are experimental EPR data, and thin lines are simulated spectra using EPR parameters described below. (i), NocL; (ii), dithionite-reduced NocL; (iii), reduced NocL plus SAM; (iv), simulated spectrum of iii, using the parameters $g_{z,y,x}$ = 2.012, 1.892, 1.798, and $L_{z,y,x}$ = 25, 36, 76 Gauss; (v), reduced NocL plus L-Trp; (vi), simulated spectra of v, which is the sum of two subspectra (vii), with the parameters $g_{z,y,x}$ = 2.023, 1.906, 1.906, and $L_{z,y,x}$ = 38, 72, 72 Gauss, and (viii), with the parameters $g_{z,y,x}$ = 2.016, 1.895, 1.846, and $L_{z,y,x}$ = 30, 16, 45 Gauss. The intensity ratio of vii and viii is 0.6: 0.4. EPR conditions used were as follows: microwave frequency, 9.390 GHz; microwave power, 1mW; modulation amplitude, 5 Gauss; modulation frequency, 100 kHz; temperature, 13K.

Fig 4. **Proposed interaction of [4Fe-4S] cluster with nucleophiles through the Fe_u site.** "X" represents non-specific ligand(s), which interacts with the [4Fe-4S] cluster to result in the heterogeneity of the [4Fe-4S] cluster of NocL. These non-specific interaction(s) will be replaced when in the presence of SAM. Colored balls show the different atoms: iron (purple), sulfur (yellow), oxygen (red), nitrogen (blue), carbon (green) and hydrogen (orange).

Fig 5. **UV-Vis absorbance spectra of reconstituted NocL.** Without the addition of dithionite (A), and with the addition of dithionite (B), dithionite plus SAM (C), and dithionite plus L-Trp (D).

Fig 6. **EPR spectra of Fe-S cluster of dithionite-reduced NocL at the different temperatures.** Without the supplementing (A), and with the supplementing L-Trp (B), and SAM (C). The EPR condition is the same as that in Fig. 3 with the annotated temperature.

Fig 7. **X-band EPR spectra of dithionite-reduced NocL for free radical identification.** Without addition of SAM and L-Trp, which serve as the background (A), and with addition of SAM plus L-Trp (B), L-[$^{2}H_{8}$]-Trp (C), and L-[1-C_{13}]-Trp (D). Spectra B, C, D are all background-subtracted. EPR conditions used were as follows: microwave frequency, 9.390 GHz; microwave power, 10μW; modulation amplitude, 2 Gauss; modulation frequency, 100 kHz; temperature, 77K. Each spectrum is the average of 80 scans.

Fig 8. **Multiple sequence alignment of ThiH subfamily radical SAM proteins**. Amino acid sequences were obtained from GenBank^{TM}, including (1) NocL from *Nocardia sp. ATCC202099*; (2) NosL from *Streptomyces. acutosus*; (3)ThiH from *Escherichia coli*; (4) ThiH from *Clostridium kluyveri* and (5) HdyG from *Clostridium kluyveri*. The blue box denotes highly conserved residues and green box denotes completely conserved amino residues. The partial conserved residues related to this study are indicated by pink or yellow box. Red and blue stars indicate the mutated residues of NocL in this study and NosL in our previous study (16), respectively.

Fig 9. **HPLC analysis of MIA production in the recombinant *E. coli* strains.** SL4151 for expressing NocL (A), SL4153 for expressing the P83A mutant NocL (B), SL4155 for expressing the M96Y mutant NocL (C), SL4161 for expressing the L245A mutant NocL (D), SL4159 for expressing the G243A mutant NocL (E), SL4163 for expressing the G247A mutant NocL (F), and SL4157 for expressing the E138A mutant NocL (G). Solid diamonds indicate an unidentified metabolite that is independent of MIA production.

Figure 1

A.

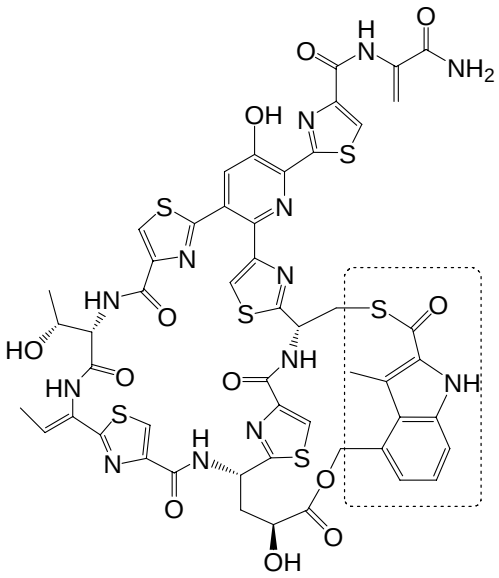

Nosiheptide (NOS)

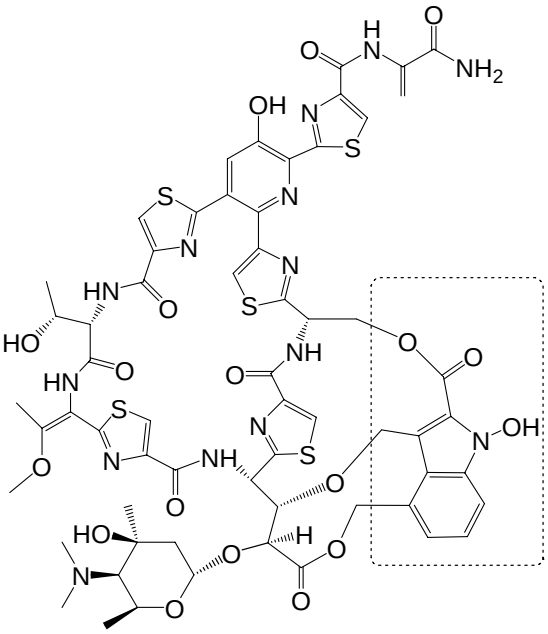

Nocathiacin I (NOC-I)

B.

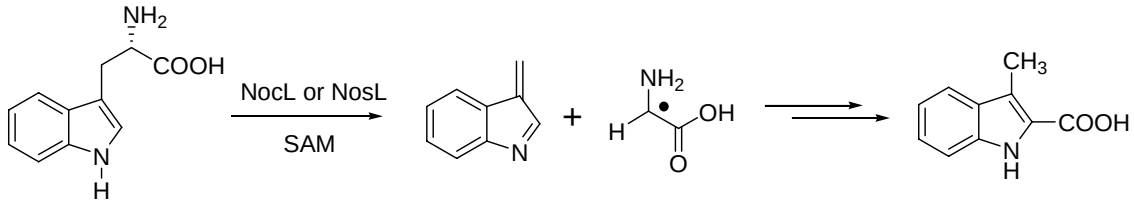

Figure 2

A.

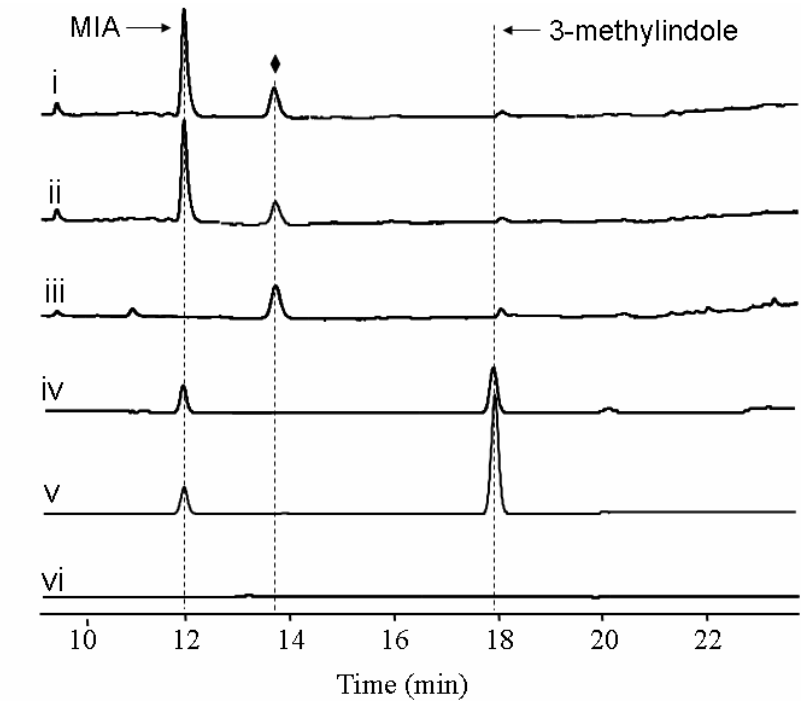
MIA
3-methylindole
i
ii
iii
iv
v
vi
10
12
14
16
18
20
22
Time (min)

B.

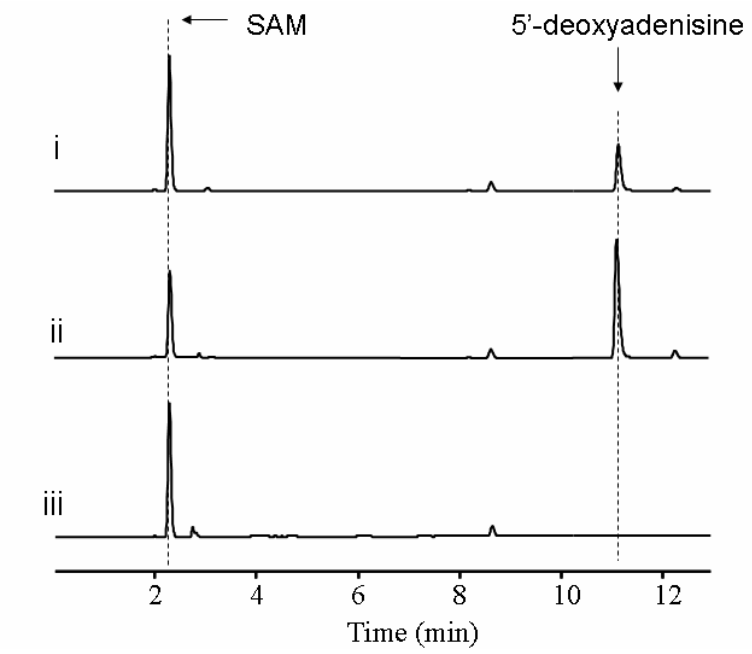
SAM
5'-deoxyadenisine
i
ii
iii
2
4
6
8
10
12
Time (min)

Figure 3

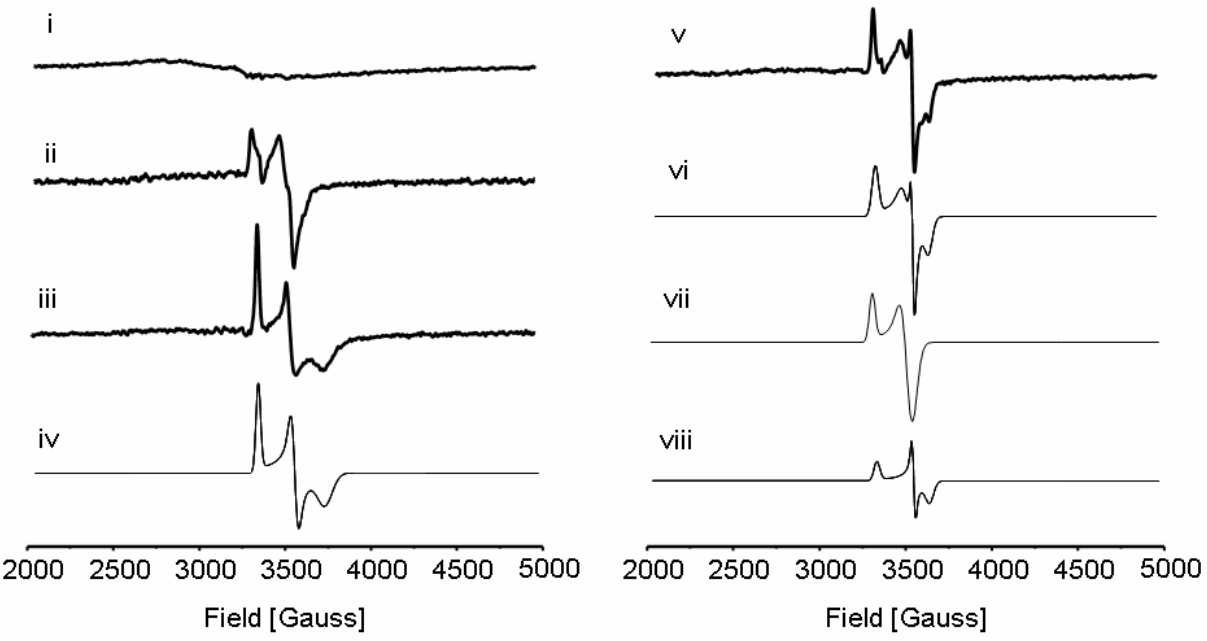
i
ii
iii
iv
2000 2500 3000 3500 4000 4500 5000
Field [Gauss]
v
vi
vii
viii
2000 2500 3000 3500 4000 4500 5000
Field [Gauss]

Figure 4

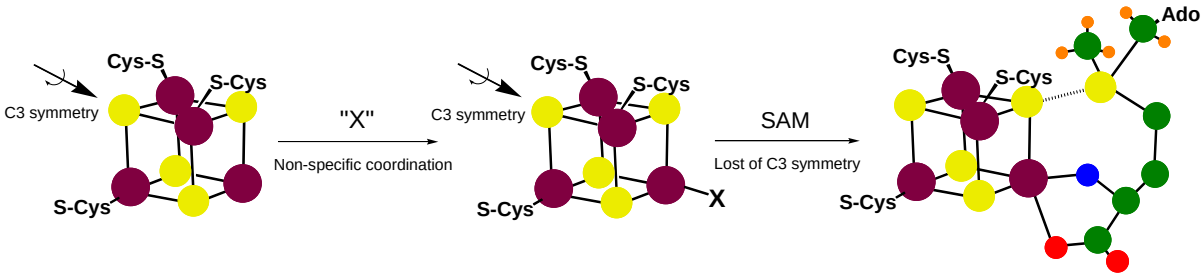
C3 symmetry
Cys-S
S-Cys
S-Cys
"X"
Non-specific coordination
C3 symmetry
Cys-S
S-Cys
S-Cys
X
SAM
Lost of C3 symmetry
Cys-S
S-Cys
S-Cys
Ado

Figure 5

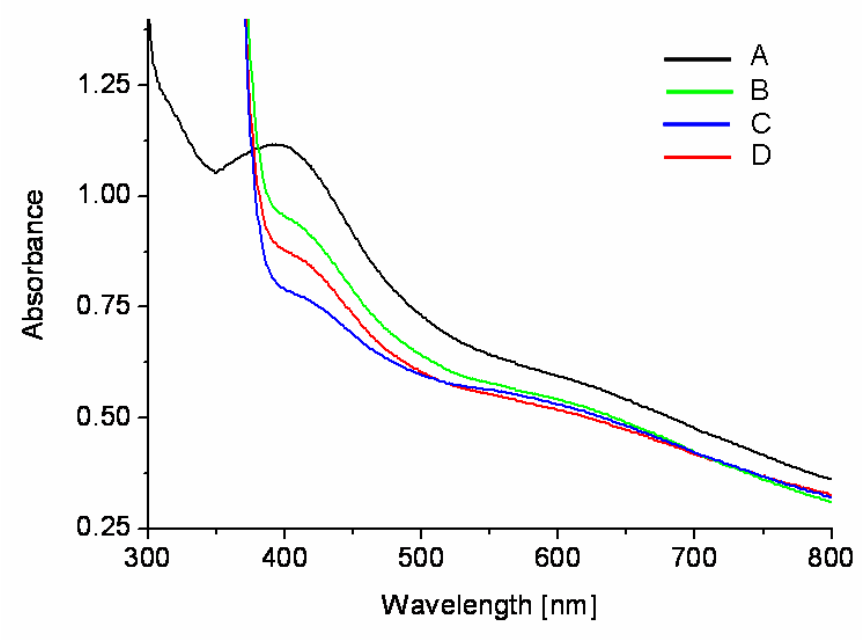
A
B
C
D
Absorbance
1.25
1.00
0.75
0.50
0.25
300
400
500
600
700
800
Wavelength [nm]

Figure 6

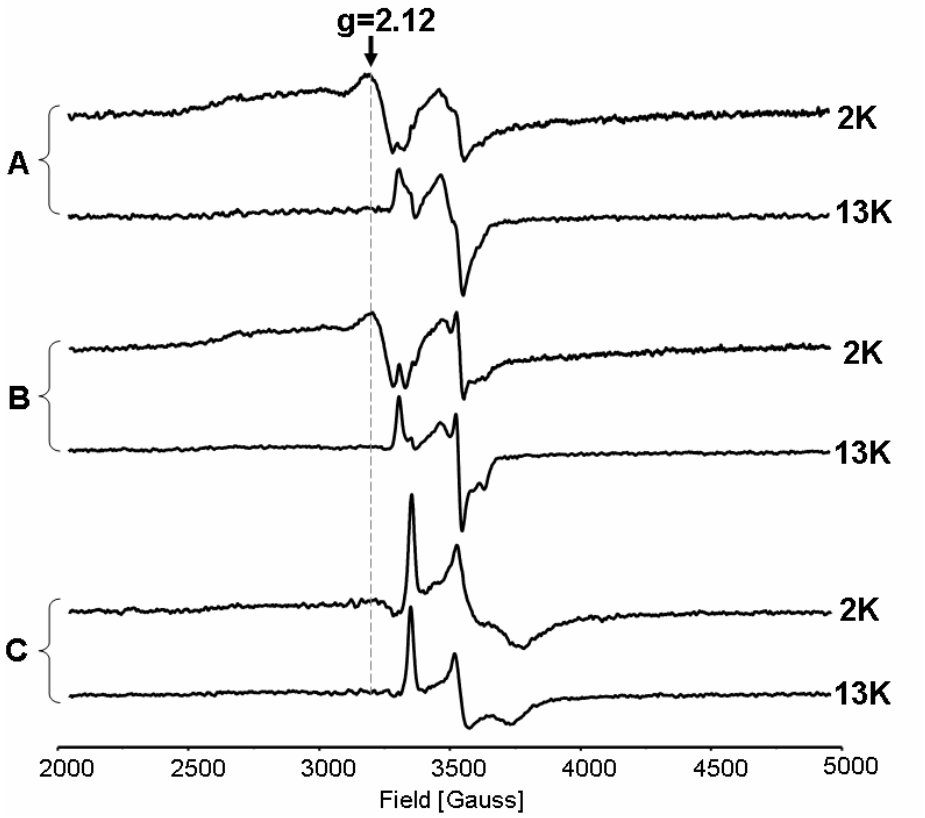
g=2.12
A
2K
13K
B
2K
13K
C
2K
13K
2000
2500
3000
3500
4000
4500
5000
Field [Gauss]

Figure 7

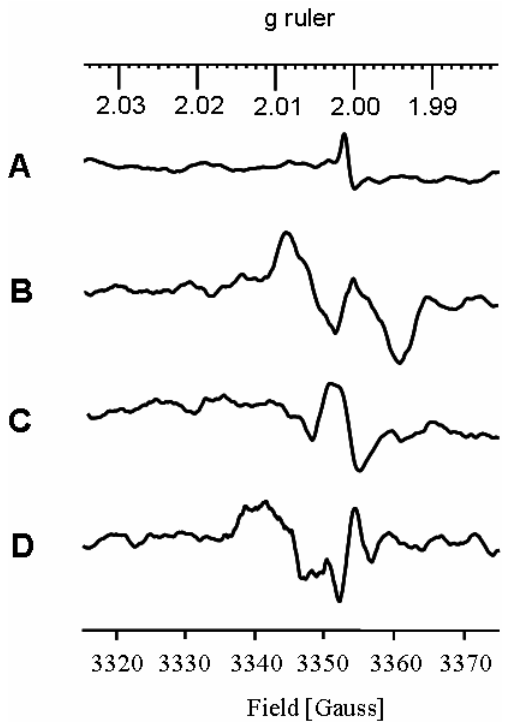
g ruler
2.03
2.02
2.01
2.00
1.99
A
B
C
D
3320
3330
3340
3350
3360
3370
Field [Gauss]

Figure 8

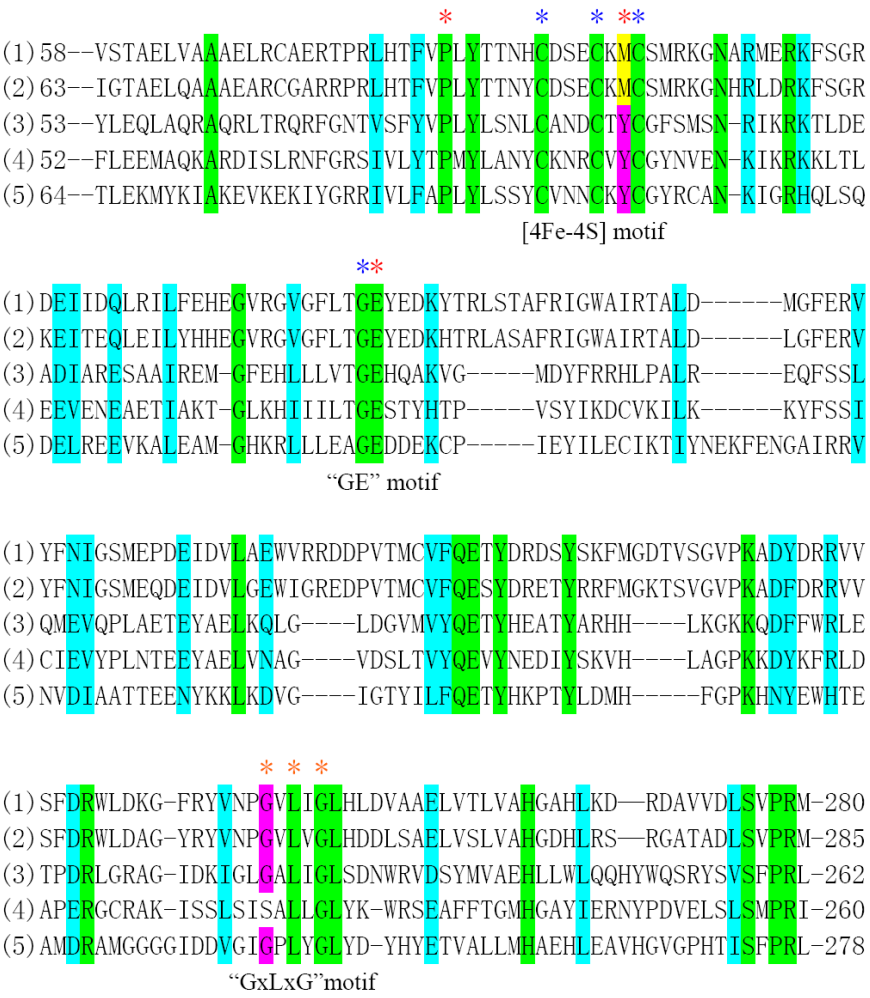
(1) 58--VSTAELVAAAELRCAERTPRLHTFVPLYTTNHCDSECKMCSMRKGNARMERKFSGR
(2) 63--IGTAELQAAAEARCGARRPRLHTFVPLYTTNYCDSECKMCSMRKGNHRLDRKFSGR
(3) 53--YLEQLAQRAQRLTRQRFGNTVSFYVPLYLSNLCANDCTYCGFSMSN-RIKRKTLDE
(4) 52--FLEEMAQKARDISLRNFGRSIVLYTPMYLANYCKNRCVYCGYNVEN-KIKRKKLTL
(5) 64--TLEKMYKIAKEVKEKIYGRRIVLFAPLYLSSYCVNNCKYCGYRCAN-KIGRHQLSQ
[4Fe-4S] motif
(1) DEIIDQLRILFEHEGVRGVGFLTGEYEDKYTRLSTAFRIGWAIRTALD------MGFERV
(2) KEITEQLEILYHHEGVRGVGFLTGEYEDKHTRLASAFRIGWAIRTALD------LGFERV
(3) ADIARESAAIREM-GFEHLLLVTGEHQAKVG-----MDYFRRHLPALR------EQFSSL
(4) EEVENEAETIAKT-GLKHIIILTGESTYHTP-----VSYIKDCVKILK------KYFSSI
(5) DELREEVKALEAM-GHKRLLLEAGEDDEKCP-----IEYILECIKTIYNEKFENGAIRRV
"GE" motif
(1) YFNIGSMEPDEIDVLAEWVRRDDPVTMCVFQETYDRDSYSKFMGDTVSGVPKADYDRRVV
(2) YFNIGSMEQDEIDVLGEWIGREDPVTMCVFQESYDRETYRRFMGKTSVGVPKADFDRRVV
(3) QMEVQPLAETEYAELKQLG----LDGVMVYQETYHEATYARHH----LKGKKQDFFWRLE
(4) CIEVYPLNTEEYAELVNAG----VDSLTVYQEVYNEDIYSKVH----LAGPKKDYKFRLD
(5) NVDIAATTEENYKKLKDVG----IGTYILFQETYHKPTYLDMH-----FGPKHNYEWHTE
(1) SFDRWLDKG-FRYVNPGVLIGLHLDVAAELVTLVAHGAHLKD--RDAVVDLSVPRM-280
(2) SFDRWLDAG-YRYVNPGVLVGLHDDLSAELVSLVAHGDHLRS--RGATADLSVPRM-285
(3) TPDRLGRAG-IDKIGLGALIGLSDNWRVDSYMVAEHLLWLQQHYWQSRYSVSFPRL-262
(4) APERGCRAK-ISSLSISALLGLYK-WRSEAFFTGMHGAYIERNYPDVELSLSMPRI-260
(5) AMDRAMGGGGIDDVGIGPLYGLYD-YHYETVALLMHAEHLEAVHGVGPHTISFPRL-278
"GxLxG"motif

Figure 9